Proceedings of the 3rd IFAC Workshop on Automatic Control in Offshore Oil and Gas Production, Esbjerg, Denmark, May 30 - June 1, 2018

We_B_Regular_Talk.1

Limitations of Topside Actuation for Rejecting Heave-induced Pressure Oscillations in Offshore Drilling

Timm Strecker [*] **Ole Morten Aamo** [*]

[*] *Department of Engineering Cybernetics, Norwegian University of Science and Technology (NTNU), Trondheim N-7491, Norway (email: timm.strecker@ntnu.no, aamo@ntnu.no)*

Abstract: The heave motion of a floating rig induces pressure oscillations in the well when the heave compensators are disabled during connections. In this paper we discuss several factors affecting the achievable performance when rejecting such pressure oscillations by feedforward by controlling the opening of the topside choke. Here, the well is modeled as a semilinear hyperbolic system with a predictor-based control law that achieves exact pressure tracking at one location in the well in the nominal case. The focus is on wells with large friction (i.e. deep wells with high-viscosity drilling muds), where large control inputs are required at the topside choke.

Keywords: Distributed-parameter system, boundary control, managed pressure drilling, disturbance rejection, feedforward control

1. INTRODUCTION

Managed pressure drilling (MPD) is a widely used method to drill wells where tight pressure control is required, as it allows to control the pressure in a well not only via the weight of the mud column but also by applying a pressure at the top of the annulus by use of an outflow choke and a backpressure pump (Hannegan, 2006). A common objective is to control the pressure at the bottom of the well to within ± 2.5 bar of a setpoint (Godhavn, 2010). Drillstring movements have long been known to induce pressure oscillations in a well that can potentially violate pressure margins (Mitchell, 1988).

When MPD is applied on a floating rig, the drillstring oscillates with the wave-induced heaving motion of the rig during connections. Over the last 5-10 years, there have been efforts at NTNU and Statoil towards designing controllers to reject the resulting pressure oscillations by controlling the opening of the topside choke. After controllers based on low-order lumped models failed to reject such high-frequency disturbances (Pavlov et al., 2010), a discretized PDE model has been presented in (Landet et al., 2013), and controllers were designed based on output regulation theory and the internal model principle . Other approaches using models obtained by system identification and controllers based on model predictive control and L_1 adaptive control, respectively, are presented in (Albert et al., 2015; Mahdianfar et al., 2016). However, these papers assume that downhole measurements are available, which is not realistic in practice. A method of designing the opening of the topside choke such that pressure oscillations are kept small by creating pressure antiresonances in the well is discussed in (Aarsnes et al., 2014). A boundary control law for a linear distributed model using only topside actuation and sensing has been developed in (Aamo, 2013).

In (Strecker et al., 2017) it has been shown that nonlinear friction can have a significant effect on the pressure oscillations. A controller design method for such semilinear hyperbolic systems is presented in (Strecker and Aamo, 2017b,c).

The main advantage of controller design methods from (Aamo, 2013) and (Strecker and Aamo, 2017b) is that they achieve exact pressure tracking at one location in the well if the model matches the actual dynamics exactly. However, due to the feedforward-nature of these control laws, high fidelity is required in the predictive capabilities of the model on which the controller design is based. Moreover, more fundamental limitations affect the achievable controller performance, related to the predictability of the disturbance/waves and to the fact that by controlling the topside choke it is only possible to reject the pressure oscillations at one location in the well. Summarizing, the following factors affect the achievable controller performance in practice

(1) uncertainty in downhole parameters, in particular in the bulk modulus and rheology of the drilling mud.
(2) errors in the wave prediction.
(3) errors in actuation due to hysteresis when opening and closing the choke.
(4) neglected dynamics of the elastic drill string.
(5) topside actuation can reject disturbances at only one location in the well, but not in a section.

For a linear model with uncertainties as described under (1)-(4), the performance of the controller from (Aamo, 2013) was investigated in (Strecker and Aamo, 2017a). In many cases, feedforward control performed better than keeping the choke opening or choke pressure constant, and it was possible to track the bottomhole pressure to within a few bar, even in presence of uncertainty. The effect of (5) is discussed in (Aarsnes et al., 2013). The focus of the
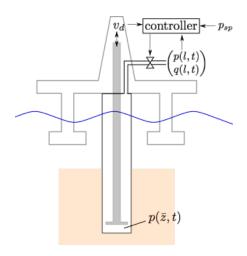
Fig. 1. Schematic of well and controller.

present paper is to investigate the effect of (1)-(5) on the pressure oscillations in a well with nonlinear friction with the controller from (Strecker and Aamo, 2017c).

The paper is organized as follows. The nominal model and the control law are introduced in Section 2. Then, the sensitivity of controller performance is investigated, first with respect to various uncertainties in isolation in Section 3 and then in a more realistic exemplary case in Section 4. Finally concluding remarks are given in Section 5.

2. NOMINAL SYSTEM

2.1 Nominal model

The controller design is based on the following model for the annular hydraulics in a vertical well, which can be derived from distributed mass and momentum balances and was first presented as a model for heave-induced pressure oscillations in (Landet et al., 2013)

$$p_t(z,t) = -\frac{\beta}{A_a} q_z(z,t) \tag{1}$$

$$q_t(z,t) = -\frac{A_a}{\rho} p_z(z,t) - \frac{1}{\rho} F(q(z,t), v_d(t)) - Ag \tag{2}$$

$$q(0,t) = -A_d v_d(t) \tag{3}$$

where $z \in [0,l]$ is the position measured from the bottom in a well of length l, $t \geq 0$ is time, $p(z,t)$ is pressure, $q(z,t)$ the volumetric flow rate, the subscripts $_z$ and $_t$ denote partial derivatives with respect to space and time, respectively, F is a nonlinear function representing friction, $v_d(t)$ is the drill string velocity, A_a the cross sectional area of the annulus, A_d is the area displaced by the drill string, β is the bulk modulus of the mud, ρ the mud density, and g the gravitational acceleration. The parameters A, β, ρ, and F can vary with z, but we omit this dependence in the notation for the sake of readability. It has been shown in (Landet et al., 2013) that (1)-(3) is capable of capturing the dynamics in an experimental well accurately. However, a very simple drilling mud was used in the experiments in (Landet et al., 2013), whereas the rheology of drilling muds used in practice is often highly nonlinear at the shear rates that occur during heave. Therefore, we adopt the methodology from (Strecker et al., 2017) for the construction of the friction term F.

The control objective is to control the pressure at $\bar{z} \in [0,l]$

(often at the bottom, i.e. $z = 0$) to a given setpoint p_{sp}, i.e.

$$p(\bar{z}, t) = p_{sp}. \tag{4}$$

The topside boundary condition can be controlled via the choke opening and backpressure pump flowrate, and is left as the control input. Moreover, we assume that both the topside pressure and flow rate, $p(l,t)$ and $q(l,t)$, are measured.

2.2 Controller

Due to the distance between actuation (topside) and the location of the tracking objective (well bottom) and due to the hyperbolic nature of (1)-(2), there is a delay before the actuation at the choke affects the pressure in the lower part of the well. The speed of sound in drilling muds is usually around $c = 1000\,\mathrm{m/s}$. In a well of several kilometers depth, the corresponding delay $d = c/l$ is in the order of several seconds, and thus in the same order of magnitude as the time period of the disturbance (heave motion). Therefore, feedforward based on the prediction of the heave motion is required to reject the disturbance. A pure feedback-based controller could react to the disturbance only after it affected the pressure and after another delay before these pressure fluctuations affect the topside measurement, and by the time the subsequent control action affects the downhole pressure the disturbance would already have changed.

The control law adopted in this paper was originally presented in (Strecker and Aamo, 2017b) and (Strecker and Aamo, 2017c). A summary of the mathematical details is given in Appendix A. It consists of the following parts

(1) a linear state transformation mapping (1)-(3) into Riemann invariants (which makes the system more convenient from a mathematical point of view)
(2) an observer estimating the distributed state using the measurements $p(l,t)$ and $q(l,t)$.
(3) a predictor mapping the observer state to the predicted state a short time into the future corresponding to the delay in the system. This predictor requires a short-term prediction of the drill string velocity v_d.
(4) a control law computing the actuation from the predicted state and predicted disturbance.
(5) a transformation mapping the output of the control law into a value for the choke opening.

Note that the control law from (Strecker and Aamo, 2017b) is computationally expensive to evaluate in practice. In this paper, however, we only use the control law to investigate the performance that can be achieved.

In order to obtain short-term predictions of the disturbance, we use a linear model for the drillstring velocity of the form

$$\dot{X}(t) = \bar{A}X(t), \qquad v_d(t) = \bar{C}X(t) \tag{5}$$

where the matrices A and C are tuned to approximate the heave spectrum and X is the state of the heave motion (e.g. heave position and velocity in case of a harmonic oscillation model). In (Fossen, 2011), chapter 8, it is suggested to determine A and C by a least-square approximation of the heave spectrum. However, we obtained better results by using a harmonic oscillation corresponding to the peak frequency ω_0 of the heave spectrum, i.e.

$l = 4000\,\mathrm{m}$	$\rho = 1500\,\mathrm{kg/m^3}$	$A_d = \pi\,r_d^2$
$r_d = 0.0635\,\mathrm{m}$	$\beta = 1.6 \times 10^9\,\mathrm{Pa}$	$A_a = \pi\,(r_w^2 - r_d^2)$
$r_w = 0.1079\,\mathrm{m}$	$\bar{x} = 0\,\mathrm{m}$	

Table 1. Nominal parameters.

$$\bar{A} = \begin{bmatrix} 0 & \omega_0 \\ -\omega_0 & 0 \end{bmatrix}, \qquad \bar{C} = [0\ 1]. \qquad (6)$$

Using more than one harmonic in A and C resulted in excessive sensitivity to noise in the measurement of v_d. Assuming that measurements of the rig velocity are available (which would perhaps require an accelerometer combined with an observer in practice), $X(t)$ can be estimated from $v_d(t)$ by the observer

$$\dot{\hat{X}}(t) = \bar{A}\hat{X}(t) + L\left(v_d(t) - \hat{v}_d(t)\right), \quad \hat{v}_d(t) = \bar{C}\hat{X}(t), \quad (7)$$

where the observer gain L is chosen such that $\bar{A} - L\bar{C}$ is Hurwitz. Then, a prediction of v_d available at time t is given by

$$\bar{v}_d^t(\theta) = \bar{C}e^{\bar{A}(\theta - t)}\hat{X}(t). \qquad (8)$$

2.3 Nominal dynamics

Throughout the paper we use the nominal parameters given in Table 1 unless stated otherwise. The drillstring with outer diameter r_d is concentric in the well of diameter r_w. The Herschel-Bulkley model is the recommended model for the rheology of drilling fluids (API Recommended Practice 13D, 2006). It relates the shear rate $\dot{\gamma}$ to the shear stress τ by

$$\begin{aligned} \tau(\dot{\gamma}) &= \left(K|\dot{\gamma}|^{n-1} + \frac{\tau_0}{|\dot{\gamma}|}\right)\dot{\gamma} && \text{if } |\tau| > \tau_0 \\ \dot{\gamma} &= 0 && \text{if } |\tau| \leq \tau_0 \end{aligned} \qquad (9)$$

where τ_0, K and n are the yield point, consistency index and flow index of the fluid, respectively. Using $\tau_0 = 5\,\mathrm{Pa}$, $K = 0.2\,\mathrm{Pas}$ and $n = 0.7$ and the geometry described above, the curve-fitting procedure from (Strecker et al., 2017) gives

$$F(q, v_d) = \sum_{i=1}^{2}\left(c_0^i + c_K^i|v_{eff}^i|^{n^i}\right)s\left(v_{eff}^i\right), \qquad (10)$$

where $v_{eff}^i = q/A - k^i v_d$,

$$c_0^1 = 2 - 1, \quad c_K^1 = 3.3, \quad n^1 = 0.7, \quad k^1 = 0.8, \qquad (11)$$
$$c_0^2 = 3.5, \qquad c_K^2 = 4.8, \quad n^2 = 0.7, \quad k^2 = 0.09, \qquad (12)$$

and

$$s(v) = \frac{v}{\sqrt{v^2 + 0.01}} \qquad (13)$$

is a smooth approximation of the sign function.

The drill string velocity v_d used in the examples, which has been obtained from on-rig measurements, is depicted in Figure 2 and compared to the estimation as given by (7) and (8) for $\theta - t = l/\sqrt{\beta/\rho}$, respectively. The estimation is very close to the true trajectory but the prediction is significantly off at some times. Note that these prediction errors are inherent to the stochastic nature of waves. The trajectory of the pressure in the well is depicted in Figure 3. For comparison purposes, the controller is switched on at $t = 100$ seconds. Before that, a constant choke opening corresponding to

$$q(l,t) = \frac{A_a}{\sqrt{\beta\rho}}(p(l,t) - (p_{sp} - \rho g\bar{x})) \qquad (14)$$
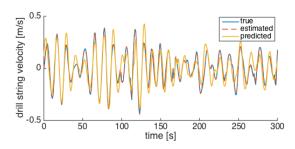

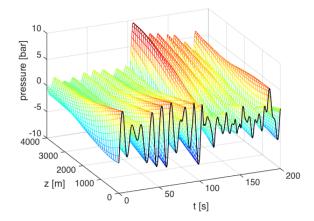Fig. 2. Drillstring velocity time series and comparison with estimated and predicted trajectory.

Fig. 3. Pressure trajectory using nominal parameters and $\bar{x} = 0$. The controller is switched on at $t = 100$, before that a constant choke opening corresponding to $q(l,t) = \frac{A_a}{\sqrt{\beta\rho}}(p(l,t) - p_{sp} + \rho gl)$ is used.

is used. We refer to (14) as impedance matching because the impedance of the outflow choke equals the impedance of the transmission line. By use of (14), pressure reflections at the choke are avoided.

In the first 100 seconds, the bit movement induces pressure oscillations at the bottom of the well and the pressure waves propagate along the well with finite speed. Due to friction, and in particular due to the yield point in (9), the pressure amplitude decays along the well. Once switched on, the controller applies a pressure at the topside choke in an attempt to cancel the downhole oscillations. Thereby, large control inputs are required at the topside choke to overcome friction and in particular to break the yield point. The mismatch between predicted and actual drillstring velocity results in non-negligible pressure oscillations at the bottom.

The pressure amplitudes are investigate closer in Figure 4. Inspired by the definition of the significant wave height of sea waves, we take the mean of the one-third highest pressure deviations from steady state (single-amplitude) for the pressure amplitude, where the pressure peaks are sampled from simulations over a 5 minute period. Because of the large control inputs, the pressure amplitudes increase with the distance from the bit. When using a noncausal controller with access to exact wave predictions (which might become implementable if additional instrumentation for the wave observation is installed), the pressure oscillations at the well bottom become zero up to numerical errors, but the pressure amplitude profile along

the well remains similar. Moving the tracking objective to $\bar{x} = 1000\,\text{m}$, for instance, rejects the oscillations at $x = 1000$ effectively but the amplitude at $x = 0$ increases slightly. This limitation is inherent if only one actuator far from where the disturbance enters the system is available, and it is impossible to control the pressure in, for instance, a section of the well.

When keeping the choke closed or the choke pressure constant, the bit-movement-induces pressure oscillations in the lower part that are, due to friction, almost independent from the choke pressure. For nominal parameters, the pressure oscillations are larger then when using active control in the lower $1000 - 2000\,\text{m}$ of the well, depending on the choice of $\bar{x}$, but smaller in the upper part.

For comparison, the pressure amplitudes in a higher viscosity mud are also depicted in Figure 4. Due to the larger friction factors, larger control inputs are required, the pressure amplitudes at the well bottom become larger, and the corresponding pressure amplitude decays are steeper.

3. SENSITIVITY OF CONTROLLER PERFORMANCE

In the following, the sensitivity of the performance with respect to various uncertainties as described in the introduction is investigated.
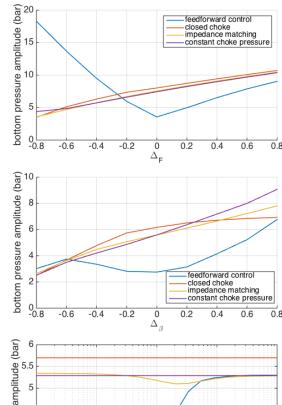
3.1 Parametric uncertainty

The main uncertainty in downhole parameters is in the bulk modulus of the drilling mud, which affects the speed of sound in the mud, and in the friction factor (which depends on the mud rheology). First, we consider multiplicative uncertainties of the form

$$F^\Delta = (1 + \Delta_F)F \qquad \beta^\Delta = (1 + \Delta_\beta)\beta \qquad (15)$$

where F^Δ and β^Δ are the uncertain plant parameters and the nominal parameters F and β as given in Table 1 are used for controller design. The sensitivity of the pressure oscillations at $x = 0$ with respect to Δ_F and Δ_β are depicted in Figures 5. The pressure oscillations are minimal if the uncertainty is zero, while without active control the pressure amplitude is monotonously increasing in both F and β. Active feedforward control performs better than keeping the choke closed, the choke pressure constant or applying impedance matching over a large range of uncertainties. Only when the friction factor is overestimated ($\Delta_F \lesssim -0.6$), the large control inputs result in excessive pressure oscillations. If friction is vastly underestimated $\Delta_F \gtrsim 1$, the control input is not enough and the performance converges to the same level as without feedforward. The results look very similar if the nominal viscosity of the mud is increased, but due to the larger control inputs, overestimating F^Δ results in even greater pressure oscillations (not depicted here).

The sensitivity with respect to Δ_β is similar in that feedforward control performs better than the other strategies for a large range of uncertainties. In the limit $\beta^\Delta \to 0$, which becomes relevant when gas is dissolved, the pressure oscillations converge to zero in all cases.

It should be mentioned that there is no formal proof for stability of the closed-loop system if there is an error between plant parameters and the parameters used for controller design, and it is unclear if one can be found and how
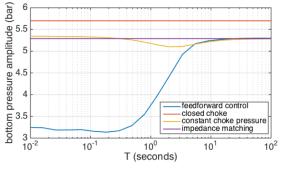

Fig. 5. Sensitivity of the performance with respect to uncertainty in friction (top), bulk modulus (middle) and the time constant of the actuator control loop (bottom).
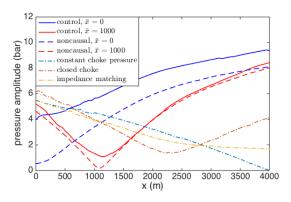
conservative the estimates on the allowable uncertainty would be. However, it can be said that the trajectories in all cases in this paper look stable. For the "passive" boundary conditions closed choke, impedance matching and constant choke pressure, stability can be proven via dissipation of energy, and it seems that the relatively large friction terms keep the system stable also in the controlled case.

3.2 Actuation errors

The models in (Aamo, 2013), (Strecker and Aamo, 2017c) assume that the topside boundary condition can be controlled with absolute precision. In practice, a separate control loop is required for the opening of the outflow choke. Hysteresis as well as the sampling rate at which the outflow can be measured limit the speed of this choke-opening control loop. To investigate the effect of this additional loop on the overall performance, we introduce an additional low-pass filter before the actuator:

$$\dot{U}_{act} = \frac{1}{T}(U_{ref} - U_{act}) \qquad (16)$$

where U_{act} represents the actual actuation entering the well, U_{ref} is the reference control input (i.e. the output of
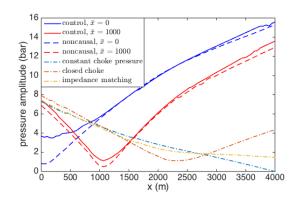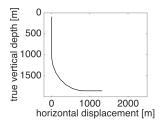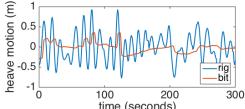
Fig. 4. Pressure amplitudes along the well when using the controller as described in Section 2.2 for $\bar{x} = 0$ and $\bar{x} = 1000$ (solid lines), when using the noncausal control law using exact wave predictions (dashed), and when using simpler choke setting without feedforward (dash-dotted): using nominal mud parameters (left) and a higher-viscosity mud with yield point 10 Pa (right)
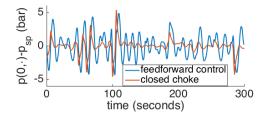

Fig. 6. Well path of a deviated well, bit and rig motion and downhole pressure oscillations.

the controller sketched in Section 2.2) and T is the time constant of the choke control loop. The sensitivity of the downhole pressure amplitude with respect to T is depicted in Figure 5 (bottom). To avoid the effect of the additional loop, T must be in the order of 0.25 seconds or faster. At $T = 1$ second, performance is affected significantly but still better than with the other topside boundary conditions, whereas the benefit of active control is lost almost completely for $T \gtrsim 5$ seconds. These numbers depend mostly on the heave spectrum and are independent from the well parameters. Keeping the choke pressure constant requires control of the choke opening, too, but the bottomhole pressure oscillations are almost independent of the time constant T because no feedforward is applied when controlling the choke pressure constant. Closed choke and impedance matching correspond to constant choke openings.
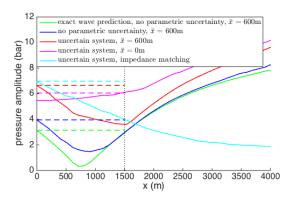
3.3 Neglected dynamics

The nominal model (1)-(3) assumes that the drillstring is rigid, which is reasonable in approximately vertical wells up to around 5000 m depth. However, the dynamics of the elastic drillstring become significant in very deep or deviated wells. The path of a 4000 m long deviated well is depicted in Figure 6. The bit movement, as calculated from the more detailed model in (Strecker et al., 2017), differs significantly from the rig motion. The figure also shows the pressure trajectory when applying the control law assuming that the string is rigid. That is, the controller tries to actively reject a predicted disturbance that differs significantly from the actual disturbance. This strategy results in significant pressure oscillations in the well, not only when the bit is not moving at all but even when

the bit moves the predictions are too erroneous. Without feedforward control, while the worst pressure peaks are in the same order of magnitude, the pressure deviation is much smaller at times when the bit is not oscillating.

While it might be possible to include the drillstring dynamics in the controller design, this will only increase the number of uncertain parameters (mechanical friction factor, etc) and it is highly questionable whether accurate enough predictions of the string movement are possible to make feedforward feasible in such a case.

4. ASSESSMENT OF ACHIEVABLE PERFORMANCE

The previous section investigated the sensitivity with respect to various modeling errors in isolation, but in practice it is highly relevant to assess the controller performance in presence of uncertainty in all parameters. Since the performance depends on a combination of several parameters, such an analysis should be done on a case-by-case basis. In the following we focus on an exemplary well with $|\Delta_F| \leq 0.3$, $|\Delta_\beta| \leq 0.2$, $T \leq 1$ second and otherwise the parameters from Table 1, and investigate the worst-case pressure oscillations in the lower 1500 m-section of the well (which can represent the case that the well is cased from 1500 m to the top), see Figure 7. In the nominal case without uncertainty in the model or wave prediction, it is optimal to locate the tracking objective at $\bar{x} = 600$ m, in which case the maximum pressure oscillations of approximately 3.2 bar are attained at both $x = 0$ and $x = 1500$ m. With uncertain wave prediction, the pressure amplitude at $x = 0$ increases to 4 bar. In presence of uncertainty in F, β and T, the pressure at the bottom can only be controlled to within ± 6.6 bar, which is significantly worse than without uncertainty. The location of the minimum
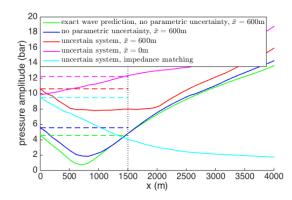
Fig. 7. Pressure amplitudes with and without uncertainty as described in text for nominal mud parameters (left) and a higher-viscosity mud with yield point 10 Pa (right).

pressure amplitude seems to move upwards in the well (to around 1500 m in this case), and it turns out that locating the tracking objective at $\bar{x} = 0$ reduces the worst-case pressure amplitude in the section slightly to about 6 bar. For both choices of $\bar{x}$, the controller performance is only slightly better than applying impedance matching at the choke which corresponds to a constant choke opening.

For comparison, the pressure amplitudes in a higher-viscosity mud with yield point 10 Pa is also depicted in Figure 7. As discussed earlier, stronger actuation is required to overcome higher friction. This increases both the pressure amplitudes in general and the sensitivity with respect to uncertainty. For the given example, the worst-case pressure amplitude grows from around 5 bar in the nominal case to, depending on $\bar{x}$, $10 - 12$ bar under the uncertainty. Moreover, impedance matching performs better than active control in this case.

5. CONCLUSIONS

We have discussed limitations in the performance of a feedforward control law rejecting heave-induced pressure oscillations by topside actuation due to model uncertainty, erroneous actuation and, more fundamentally, related to uncertain disturbance prediction and the fact that the pressure at only one location can be controlled. In many situations, active feedforward control brings an improvement compared to keeping the choke opening or choke pressure constant. However, large control inputs are required at the choke to overcome friction in high-viscosity muds, making the pressure amplitude decay along the well steep and the performance sensitive to uncertainty. Notably, the remaining pressure amplitudes are larger than in the small-friction case that has been considered in (Strecker and Aamo, 2017a). In practice, a case study like in Section 4 can help to decide not only the best control strategy but also if the achievable performance is satisfactory, or if drilling should be suspended to wait for better weather/wave conditions.

While it is advisable to assess the controller performance on a case-by-case basis, the pressure oscillations tend to increase with well length, mud viscosity, parametric uncertainty, actuation errors, heave prediction errors and the length of the section in which the pressure oscillations are to be rejected, and decrease with well diameter.

The control law employed in this paper is designed to exactly reject disturbances at one location under nominal conditions but, since the figures in Figure 5 are relatively symmetric with respect to $\Delta_{F/\beta} = 0$ for small uncertainties, it is unclear if it is possible to find a controller that performs (significantly) better under uncertainty. In this regard, the optimal control law would be obtained by minimizing the worst-case pressure oscillations under uncertainty, perhaps by solving an optimization problem of the form

$$\min_C \left(\max_{\delta \in \Delta, x \in X} p_{amp}(x, \delta, C) \right) \qquad (17)$$

where C represents the control law and $p_{amp}(x, \delta, C)$ is the closed-loop pressure amplitude at location x for uncertainty δ. Considering the nonlinear and distributed nature of the system (1)-(2) it is, however, unclear if a solution to optimal control problem (17) can be found. Moreover, while such an optimal controller might improve the sensitivity with respect to parametric uncertainty to some degree, limitations related to wave prediction and the pressure amplitude profile along a section are more fundamental and cannot be removed by topside control.

Finally, pressure control performance could be improved by two ways . Relying on topside actuation as presented in this paper, better performance can be enabled by a more accurate heave prediction. If additional instrumentation is installed to observe the wave motion in a certain distance around the rig (for instance by installing a ring of buoys around the rig or an optical/radar-based method for wave observation), combined with a model for the rig's motion response, more accurate heave predictions than what is achieved by (7)-(8) would enable a controller performance closer to that of the noncausal controller in Figure 4. However, limitations due to parametric uncertainty and due to the pressure amplitude profile along the well would remain. If very tight pressure control is required in challenging wells, an alternative approach would be to maintain circulation and install a controllable valve in the BHA to directly control the downhole inflow into the annulus. By placing actuator and sensors directly at the well bottom where pressure control is required, measurements and actuation no longer have to propagate through the whole mud column. Thus, no heave prediction is required, and sensitivity with respect to uncertainty in mud parameters can be expected to be reduced significantly.

REFERENCES

Aamo, O.M. (2013). Disturbance rejection in 2 x 2 linear hyperbolic systems. *IEEE Transactions on Automatic Control*, 58(5), 1095–1106.

Aarsnes, U.J.F., Aamo, O.M., Hauge, E., and Pavlov, A. (2013). Limits of controller performance in the heave disturbance attenuation problem. In *2013 European Control Conference (ECC)*, 1071–1076.

Aarsnes, U.J.F., Gleditsch, M.S., Aamo, O.M., and Pavlov, A. (2014). Modeling and avoidance of heave-induced resonances in offshore drilling. *SPE Drilling & Completion*, 29(04), 454–464.

Albert, A., Aamo, O.M., Godhavn, J.M., and Pavlov, A. (2015). Suppressing pressure oscillations in offshore drilling: Control design and experimental results. *IEEE Transactions on Control Systems Technology*, 23(2), 813–819.

API Recommended Practice 13D (2006). Rheology and hydraulics of oil-well drilling fluids.

Fossen, T.I. (2011). *Handbook of marine craft hydrodynamics and motion control.* John Wiley & Sons.

Godhavn, J.M. (2010). Control requirements for automatic managed pressure drilling system. *SPE Drilling & Completion*, 25(03), 336–345.

Hannegan, D.M. (2006). Case studies-offshore managed pressure drilling. In *SPE Annual Technical Conference and Exhibition*. Society of Petroleum Engineers.

Landet, I.S., Pavlov, A., and Aamo, O.M. (2013). Modeling and control of heave-induced pressure fluctuations in managed pressure drilling. *IEEE Transactions on Control Systems Technology*, 21(4), 1340–1351.

Mahdianfar, H., Hovakimyan, N., Pavlov, A., and Aamo, O.M. (2016). L 1 adaptive output regulator design with application to managed pressure drilling. *Journal of Process Control*, 42, 1–13.

Mitchell, R. (1988). Dynamic surge/swab pressure predictions. *SPE drilling engineering*, 3(03), 325–333.

Pavlov, A., Kaasa, G.O., and Imsland, L. (2010). Experimental disturbance rejection on a full-scale drilling rig. *IFAC Proceedings Volumes*, 43(14), 1338–1343.

Strecker, T. and Aamo, O.M. (2017a). Frequency domain analysis of backstepping-based disturbance rejection in a linear hyperbolic system. In *Australian & New Zealand Control Conference*.

Strecker, T. and Aamo, O.M. (2017b). Output feedback boundary control of 2×2 semilinear hyperbolic systems. *Automatica*, 83, 290–302.

Strecker, T. and Aamo, O.M. (2017c). Rejecting heave-induced pressure oscillations in a semilinear hyperbolic well model. In *American Control Conference (ACC), 2017*, 1163–1168. IEEE.

Strecker, T., Aamo, O.M., and Manum, H. (2017). Simulation of heave-induced pressure oscillations in herschel-bulkley muds. *SPE Journal*.

Appendix A. SUMMARY OF CONTROL LAW

In the following we briefly summarize the control law which is given in detail in (Strecker and Aamo, 2017b) and (Strecker and Aamo, 2017c). See also Figure A.1.
After rescaling the domain to $x = z/l$ (with $\bar{x} = \bar{z}/l$), the state transformation given in (Strecker and Aamo, 2017c) maps (1)-(3) into
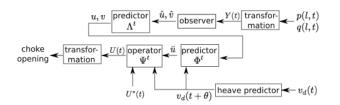

Fig. A.1. Controller structure.

$$u_t(x,t) = -\epsilon_u u_x(x,t) + F_u(u(x,t), v(x,t), v_d(t)), \quad \text{(A.1)}$$
$$v_t(x,t) = \epsilon_v v_x(x,t) + F_v(u(x,t), v(x,t), v_d(t)), \quad \text{(A.2)}$$
$$u(0,t) = -v(0,t) - A_d v_d(t), \quad \text{(A.3)}$$
$$v(1,t) = U(t), \qquad Y(t) = u(1,t), \quad \text{(A.4)}$$

where U is the actuation, Y the measurement and all other coefficients are given in (Strecker and Aamo, 2017c). In terms of the original physical system, we have

$$U(t) = \frac{1}{2}\left(q(l,t) - \frac{A}{\sqrt{\beta\rho}}(p(l,t) - p_{sp} + \rho g(l - \bar{z}))\right)$$

$$Y(t) = \frac{1}{2}\left(q(l,t) + \frac{A}{\sqrt{\beta\rho}}(p(l,t) - p_{sp} + \rho g(l - \bar{z}))\right)$$

The control objective becomes

$$u(\bar{x},t) = v(\bar{x},t). \quad \text{(A.5)}$$

Define

$$\phi_v(x) = \int_x^1 \frac{1}{\epsilon_v(\xi)}d\xi, \qquad \phi_u(x) = \int_x^1 \frac{1}{\epsilon_u(\xi)}d\xi,$$
$$\bar{u}(x,t) = u(x, t + \phi_v(x,t)), \quad \bar{v}(x,t) = v(x, t + \phi_v(x,t)),$$
$$\check{u}(x,t) = u(x, t - \phi_u(x,t)), \quad \check{v}(x,t) = v(x, t - \phi_u(x,t)).$$

Consider the observer

$$\hat{u}_x(x,t) = \frac{1}{\epsilon_u}F_u(\hat{u}(x,t), \hat{v}(x,t), v_d(t - \phi_u(x,t))), \quad \text{(A.6)}$$

$$\hat{v}_t(x,t) = \frac{\epsilon_u \epsilon_v}{\epsilon_u + \epsilon_v}\hat{v}_x(x,t) \quad \text{(A.7)}$$
$$\qquad + \frac{\epsilon_u}{\epsilon_u + \epsilon_v}F_v(\hat{u}(x,t), \hat{v}(x,t), v_d(t - \phi_u(x,t))),$$

$$\hat{u}(1,t) = Y(t), \qquad \hat{v}(1,t) = U(t), \quad \text{(A.8)}$$

with arbitrary bounded initial guess. For each t there exists an prediction operator Λ^t, independent of $U(t)$, such that for all $t \geq \phi_u(0) + \phi_v(0)$

$$(u(\cdot,t), v(\cdot,t)) = \Lambda^t(\hat{u}(\cdot,t), \hat{v}(\cdot,t)). \quad \text{(A.9)}$$

Moreover, for every t there exists an prediction operator Φ^t, independent of $U(t)$ but depending on the predicted values $v_d(t + \theta)$ for $\theta \in [0, \phi_v(0)]$, such that

$$\bar{u}(\cdot,t) = \Phi^t(u(\cdot,t), v(\cdot,t)). \quad \text{(A.10)}$$

$\bar{v}(\cdot,t)$ satisfies

$$\bar{v}_x(x,t) = -\frac{1}{\epsilon_v}F_v(\bar{u}(x,t), \bar{v}(x,t), v_d(t + \phi_v(x,t))). \quad \text{(A.11)}$$

Next we determine the desired $\bar{v}(\bar{x},t)$, which we denote by $U^*(t)$. If $\bar{x} = 0$, inserting (A.3) into (A.5) gives $U^*(t) = \frac{1}{2}d(t + \phi_v(0))$. If $\bar{x} \neq 0$, $U^*(t) = \bar{u}(\bar{x},t)$ where $\bar{u}(\bar{x},t)$ is given by the evaluation of Φ^t. The required $U(t)$ to achieve $\bar{v}(\bar{x},t) = U^*(t)$ is determined by solving (A.11) backwards, i.e. solving the Cauchy problem

$$\varphi_x(x) = -\frac{1}{\epsilon_v}F_v(\bar{u}(x,t), \varphi(x), v_d(t + \phi_v(x,t))), \quad \text{(A.12)}$$

with $\varphi(\bar{x}) = U^*(t)$ for $x \in [\bar{x}, 1]$ and setting $U(t) = \varphi(1)$, and defining the operator

$$\Psi^t : (\bar{u}(\cdot,t), U^*(t)) \mapsto \varphi(1). \quad \text{(A.13)}$$